HHS Public Access

Author manuscript

J Neurosci Res. Author manuscript; available in PMC 2018 September 01.

Published in final edited form as:

J Neurosci Res. 2018 March ; 96(3): 436–448. doi:10.1002/jnr.24183.

Glial fibrillary acidic protein promoter determines transgene expression in satellite glial cells following intraganglionic adeno-associated virus delivery in adult rats

Hongfei Xiang[1,2,¶], **Hao Xu**[1,2,¶], **Fan Fan**[3], **Seung-Min Shin**[1], **Quinn H. Hogan**[1,4], and **Hongwei Yu**[1,4]

[1]Department of Anesthesiology, Medical College of Wisconsin, Milwaukee, Wisconsin 53226, United States of America

[2]Department of Orthopedic Surgery, Affiliated Hospital of Qingdao University, Qingdao 266000, People's Republic of China

[3]Department of Pharmacology and Toxicology, Mississippi University Medical Center, Jackson, Mississippi 39216, United States of America

[4]Zablocki Veterans Affairs Medical Center, Milwaukee, Wisconsin 53295, United States of America

Abstract

Recombinant adeno-associated viral (AAV)-mediated therapeutic gene transfer to dorsal root ganglia (DRG) is an effective and safe tool for treating chronic pain. However, AAV with various constitutively active promoters leads to transgene expression predominantly to neurons while glial cells are refractory to AAV transduction in the peripheral nervous system. The present study evaluated whether *in vivo* satellite glial cells (SGC) transduction in the DRGs can be enhanced by the SGC-specific GFAP promoter and by using shH10 and shH19 that are engineered capsid variants with Müller glia-prone transduction. Titer-matched AAV6 (as control), AAVshH10, and AAVshH19, all encoding the EGFP driven by the constitutively active CMV promoter, as well as AAV6-EGFP and AAVshH10-EGFP driven by a GFAP promoter (AAV6-GFAP-EGFP and AAVshH10-GFAP-EGFP) were injected into DRGs of adult male rats. Neurotropism of gene expression was determined and compared by immunohistochemistry. Results showed that injection of AAV6- and AAVshH10-GFAP-EGFP induces robust EGFP expression selectively in SGCs, whereas injection of either AAVshH10-CMV-EGFP or AAVshH19-CMV-EGFP into DRGs resulted in a similar *in vivo* transduction profile to AAV6-CMV-EGFP, all showing efficient transduction of sensory neurons without significant transduction of glial cell populations. Co-

Correspondence author: Hongwei Yu, MD; Department of Anesthesiology, Medical College of Wisconsin, 8701 Watertown Plank Road, Milwaukee, WI 53226; Phone: (414) 955-5745, Fax: (414) 955-6507, hyu@mcw.edu.
¶These authors contributed equally to this work.

CONFLICT OF INTEREST STATEMENT

The authors have no competing interests.

AUTHOR'S ROLEs

Conceptualization: HY and QHH. Funding acquisition: QHH. Experiment design: HY. Investigation: HFX, HX, FF, HY, DC. Writing the manuscript: HY and QHH. All authors had full access to all the data in the study and take responsibility for the integrity of the data and the accuracy of the data analysis.

injection of AAV6-CMV-mCherry and AAV6-GFAP-EGFP induces transgene expression in neurons and SGCs separately. This report, together with our prior studies, demonstrates that the GFAP promoter rather than capsid tropism determines selective gene expression in SGCs following intraganglionic AAV delivery in adult rats. A dual AAV system, one with GFAP promoter and the other with CMV promoter, can efficiently express transgenes selectively in neurons vs. SGCs.

Graphical abstract

This study demonstrates that AAV vectors with a GFAP promoter are capable of discriminating for SGC transduction when delivered into the DRG.

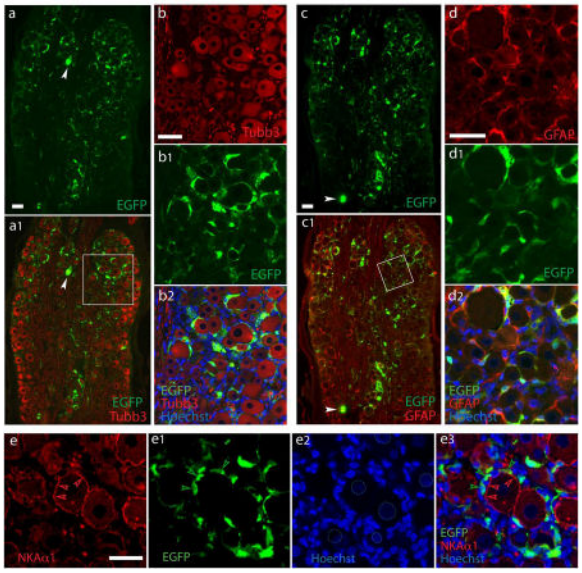

Keywords

Recombinant adeno-associated virus; Gene therapy; Dorsal root ganglion; Satellite glial cells; Pain

INTRODUCTION

Ganglionic SGCs are an important element in the pain signaling pathways (Hanani, 2005; Scholz and Woolf, 2007). SGCs proliferation and activation following nerve injury influences sensory processing by various mechanisms including alteration of gene expression, increased coupling between SGCs and between SGCs and neurons, and chemokines/cytokines release that induces microglia activation (Liu and Yuan, 2014; McMahon and Malcangio, 2009; Milligan and Watkins, 2009; Watkins and Maier, 2003). Genetic manipulation of SGC-specific molecules such as connexin 43 (Cx43) (Ohara et al., 2008), glutamine synthase (GS) (Jasmin et al., 2010), ATP-sensitive inward rectifier potassium channel 10 ($kir_{4.1}$) (Vit et al., 2008), excitatory amino acid transporter 1 (EAAT1) (Jasmin et al., 2010), purinergic ionotropic P2X7 receptor (P2X7R) (Chen et al., 2008), as well as GFAP (Kim et al., 2009), can substantially alter sensory responses in normal and nerve-injured rodents. Thus, therapeutic gene modulation specifically targeting the SCGs

population in DRG could offer new opportunities for chronic pain treatment (Gao and Ji, 2010; Jasmin et al., 2010; McMahon and Malcangio, 2009).

Gene therapy has demonstrated a potential for novel treatments for chronic pain. In preclinical studies, gene delivery by use of AAV has been established as an efficient tool for gene transfer into post-mitotic peripheral sensory neurons and for long-term control of neuropathic pain with minimal toxicity (Asokan et al., 2012; Beutler and Reinhardt, 2009; Beutler, 2010; Mason et al., 2010; Yu et al., 2013). The capsid protein and the promoter are major determinants of AAV tropism to different cell types. The natural tropism of AAV vectors based on the widely used AAV2 genome with constitutively active promoters and pseudotyped with various serotype capsids leads predominantly to neuronal transduction. Although variable, low level of non-selective SGCs transduction *in vivo* after intraganglionic delivery has been reported, the use of AAV to transduce SGCs has generally resulted in limited success in adult animals (Asokan et al., 2012; Beutler and Reinhardt, 2009; Beutler, 2010; Mason et al., 2010; Yu et al., 2013). This view has been challenged in the central nervous system (CNS) by showing that use of a GFAP promoter increases the astrocyte transduction of AAV-mediated transgene expression (von Jonquieres et al., 2013). However, whether GFAP promoter determines glial cell transduction in DRG has not been reported. Capsid protein is another important determinant for AAV tropism. AAVshH10 (an AAV6 capsid variant) and AAVshH19 (an AAV2 capsid variant) are recently engineered novel AAV capsids that provide efficient Müller glia-permissive gene expression (Dalkara et al., 2011; Klimczak et al., 2009; Koerber et al., 2009; Zolotukhin et al., 2013). It is not clear, however, whether these AAV capsid mutants can be adopted for gene transfer to ganglionic SGCs.

The purpose of this study was to evaluate whether cell-specificity for the SGC transduction in DRG could be enhanced using AAVshH10 and AAVshH19 capsids, and transgene-driven by SGC-specific GFAP promoter. Our work establishes that GFAP promoter is effective in providing SGC-selective transgene expression following intraganglionic AAV delivery in adult rats, and this strategy should prove useful for the development of gene expression systems targeting SGC signaling for chronic pain.

MATERIALS AND METHODS

Experimental animals

Adult male Sprague Dawley (SD) rats weighing 125–150 g body weight (Charles River Laboratories, Wilmington, MA) were used. All animal experiments were performed with the approval of the Zablocki VA Medical Center Animal Studies Subcommittee and Medical College of Wisconsin Institutional Animal Care and Use Committee (Permit number: 3690-03) in accordance with the National Institutes of Health Guidelines for the Care and Use of Laboratory Animals. Animals were housed individually in a room maintained at constant temperature (22±0.5°C) and relative humidity (60±15%) with an alternating 12h light-dark cycle. Animals were access to water and food *ad libitum* throughout the experiment, and all efforts were made to minimize suffering.

AAV production

AAV vectors were produced and purified in our laboratory by previously described methods (Yu et al., 2013). This included AAV particle purification by optiprep ultracentrifugation and concentration by use of Centricon Plus-20 (Regenerated Cellulose 100,000 MWCO, Millipore, Billerica, MA). AAV titer was determined by PicoGreen (life technologies, Carlsbad, CA) assay, and final aliquots were kept in 1x phosphate buffered saline (PBS) containing 5% sorbitol (Sigma–Aldrich, St. Louis, MO) and stored at −80°C. Plasmids of capsid AAV6 and two glia-prone capsid variants (AAVshH10 and AAVshH19) were utilized as reported in previous publication (Koerber et al., 2009; Yu et al., 2013). pAAV-GFAP-EGFP shuttle plasmid (containing a compact GFAP promoter, 694bp gfaABC1D) was purchased from Addgene (plasmid#: 50473, Cambridge, MA). The gfaABC1D promoter is suitable for packaging into AAV vectors, and has been reported to have essentially the same expression pattern as the full GFAP promoter (Lee et al., 2008). Five different AAVs were prepared: AAV2/6 expressing EGFP driven by the CMV or GFAP promoter (subsequently referred to as AAV6-CMV-EGFP and AAV6-GFAP-EGFP), and two Müller glia-prone capsid-mutant vectors with the same AAV expressing EGFP by CMV promoter but packaged with capsids shH10 and shH19 and by GFAP promoter with capsid shH10 (subsequently referred to as AAVshH10-CMV-EGFP, AAVshH19-CMV-EGFP, and AAVshH10-GFAP-EGFP). The titers (GC/ml) of AAV6-CMV-EGFP, AAV6-GFAP-EGFP, AAVshH10-CMV-EGFP, AAVshH19-CMV-EGFP, and AAVshH10-GFAP-EGFP vectors were 1.0×10^{13}, 2.19×10^{13}, 1.89×10^{13}, 2.26×10^{13}, 1.58×10^{13}, respectively. The same lot of viral preparation was used for all *in vivo* experiment. Vectors were evaluated for purity by sodium dodecyl sulfate-polyacrylamide gel (SDS-PAGE) electrophoresis followed by silver stain using a Pierce silver stain kit (Fisher Scientific, Rockford, IL) according to manufacturer's protocol (Supporting Fig. 1). An AAV6-CMV-mCherry with titer of 1.21×10^{13} GC/ml was purchased from Vigene Biosciences (Rockville, MD).

Injection of AAV vectors into the DRGs

AAV vectors were microinjected into right lumbar (L) 4 and L5 DRGs of isoflurane-anesthetized rats, performed through a micropipette using previously described techniques (Fischer et al., 2011). Briefly, the surgically exposed intervertebral foramen was minimally enlarged by removal of laminar bone. Injection was performed through a micropipette that was advanced ~100 μm into the ganglion. Rats received L4 and L5 DRG injections of vectors (one vector per rat), consisting of 2 μl with adjusted titers containing a total of 2.0×10^{10} genome containing viral particles. For dual AAV vector injection, 1 μl of AAV6-GFAP-EGFP was mixed with 1 μl of AAV6-CMV-mCherry. Injection was performed over a 5-min period using a Nanoliter 2000 microprocessor-controlled injector (World Precision Instruments, Sarasota, FL, USA). Removal of the pipette was delayed for an additional 5 min to minimize the extrusion of the injectate. Following the injection and closure of overlying muscle and skin, the animals were returned to the animal house where they remained for 5 weeks. In other animals, sham injection was performed, with exposure of the DRGs but no injection.

Behavioral testing (Fischer et al., 2011)

Mechanical withdrawal threshold testing (von Frey) was performed using calibrated monofilaments (Patterson Medical, Bolingbrook, Illinois, USA). Briefly, beginning with the 2.8 g filament, filaments were applied with just enough force to bend the fiber and held for 1 s. If a response was observed, the next smaller filament was applied, and if no response was observed, the next larger was applied, until a reversal occurred, defined as a withdrawal after a previous lack of withdrawal, or vice versa. Following a reversal event, four more stimulations were performed following the same pattern. The forces of the filaments before and after the reversal, and the four filaments applied following the reversal, were used to calculate the 50% withdrawal threshold (Chaplan et al., 1994). Rats not responding to any filament were assigned a score of 25 g. Heat nociception (Hargreaves test) was performed using a device designed for the purpose of identifying heat sensitivity (Paw Thermal Stimulator System, University Anesthesia Research & Development Group, San Diego, CA). Rats were placed on a temperature-regulated glass platform heated to 30°C and the lateral plantar surface of hind paws stimulated with a radiant heat source (50 W halogen bulb) directed through an aperture. The time elapsed from initiation of the stimulus until withdrawal (withdrawal latency) as detected by a series of photocells was measured. Each hind paw was tested 4 times and the withdrawal latency values averaged.

Characterization of neurotropism of intraganglionic AAV-mediated transgene expression

Five weeks after injection, animals were terminally anesthetized. DRGs were dissected, post-fixed in 4% PFA, and processed for paraffin embedding and sectioning. Double immunolabeling histochemistry (IHC) was performed to characterize cellular specificity and distribution of target molecules in sections, as described in a previous publication (Yu et al., 2011). In brief, 5μm-thick sections were deparaffinized and rehydrated through graded alcohol. Sections were immunolabeled with the selected primary antibodies (Table 1). All antibodies were diluted in 1x phosphate buffered saline (PBS), containing 0.05% Triton X-100 and 3% bovine serum albumin (BSA). Normal immunoglobulin G (IgG from same species as the first antibody) was replaced for the first antibody as the negative controls (Table 1). The appropriate fluorophore-conjugated (A1exa 488 or A1exa 594, 1:2000) secondary antibodies (Jackson ImmunoResearch, West Grove, PA) were used to reveal immune complexes. The sections were washed three times 5min each with PBS containing 0.05% tween 20 between incubations. To stain nuclei, l.0μg/ml Hoechst 33342 (life technologies) was added to the secondary antibody mixture. The sections were examined and images acquired on a Nikon TE2000-S fluorescence microscope (El Segundo, CA), equipped with an Optronics QuantiFire digital camera and acquisition software (Ontario, NY), as well as filters suitable for selectively detecting the green, red and blue fluorescence. For each comparative experiment, all images were acquired with identical settings for detector gain and under a 10× objective with 0.5 numerical aperture at 2048×2048 pixel resolution. For double-label colocalization, images from the same section but showing different antigen signals were overlaid.

Intensity Correlation Analysis was performed to determine co-expression of EGFP with glial markers in SGCs as previously described (Li et al., 2004) using ImageJ Software. In brief, fluorescence intensity was quantified in matched ROIs (the green and red colors varied in

close synchrony) for each pair of images. Mean background was determined from areas outside the section regions and was subtracted from each file. On the basis of the algorithm, in an image where the intensities vary together, the product of the differences from the mean (PDM) will be positive. If the pixel intensities vary asynchronously (the channels are segregated), then most of the PDM will be negative. The intensity correlation quotient (ICQ) is based on the nonparametric sign-test analysis of the PDM values and is equal to the ratio of the number of positive PDM values to the total number of pixel values. The ICQ values are distributed between −0.5 and +0.5 by subtracting 0.5 from this ratio. In random staining, the ICQ approximates 0. In segregated staining, ICQ is less than 0; while for dependent staining, ICQ is greater than 0.

Quantification of transgene expression in neurons or SGCs was determined as reported previously (Puljak et al., 2009; Yu et al., 2013). Immunostaining of Tubb3 (a pan neuronal marker) and GFAP or GS (SGC markers) were used to distinguish neurons and SGCs, respectively. Neurons and SGCs can also be distinguished in Hoechst counterstain; neuronal nuclei are larger and less intensively stained compared with SGC nuclei (Wang et al., 2016). Neurons that were surrounded by EGFP-positive SGC rings co-labeled with GFAP or GS by more than 50% of their circumference were counted and expressed as a percentage of neurons with EGFP-positive SGC rings per total neurons present in the fields (Nascimento et al., 2014). EGFP-positive neurons were defined as the neurons with the fluorescence intensity greater than average background fluorescence plus 2 standard deviations of neurons in a section from a naive animal (no vector injection) under identical acquisition parameters (Yu et al., 2013).

Western blotting (Wang et al., 2016)

Lysates of HEK293T cells and DRG tissues were extracted using 1× RIPA buffer (20 mm Tris-HCl pH 7.4, 150 mm NaCl, 1% Nonidet P-40, 1% sodium deoxycholate, 0.1% SDS, with 0.1% Triton X100 and protease inhibitor cocktail). Protein concentration determined by using the BCA kit (Pierce, Rockford, IL). Western blotting of cell lysates or tissue homogenates (20 μg protein) was preceded by SDS-PAGE gel electrophoresis, transferred onto nitrocellulose, and probed with a polyclonal rabbit anti-GFP antibody (1:1,000; Cell Signaling, Danvers, MA), rabbit anti-mCherry antibody (1:500, life technologies), or anti-GFAP (1:1000, Dako). Immunoreactive proteins were detected by enhanced chemiluminescence (Pierce, Rockford, IL) after incubation with HRP-conjugated second antibodies (1:2000, SCB) and exposed to photographic film. GAPDH was used as a loading control. Ratios of the band density of GFAP protein to the GAPDH were calculated and the percentage changes of GFAP in the sham and the injected DRG samples were normalized against the average of naive samples.

Statistics

All statistical analysis was performed using Prism (GraphPad Software, La Jolla, CA). Behavioral changes over time were analyzed by repeated measures parametric 2-way ANOVA for von Frey and heat tests, followed by Tukey's *post hoc* test for multiple comparisons. The differences of EGFP-positive SGC rings or neuronal soma for each vector, as well as GFAP expression in DRGs by Western blots were analyzed using oneway

ANOVA. Results are reported as mean ± standard error of the mean (SEM). $P<0.05$ were considered statistically significant. Significance of ICQs of EGFP with Hmgcs1 or Iba1 was tested by means of the normal approximation of the nonparametric Wilcoxon Rank test (Li et al., 2004).

RESULTS

GFAP promoter restricts AAV6-mediated transgene expression to SGCs

We initially tested the properties of AAV with the GFAP promoter, compared to the CMV promoter, in expressing a transgene in SGCs after delivery to the DRGs. Both CMV and GFAP promoters driving the EGFP gene were packaged into AAV6 vectors with a single-stranded AAV2 genome. Animals were euthanized 5 weeks after administration, DRG sectioned, and cell specificity of EGFP expression was analyzed by immunofluorescence using GFP antibodies for which the specificity to detect EGFP expression in sections was verified (cf Supporting Fig. 2a and 3). Similar to our previous report (Yu et al., 2013; Yu et al., 2016), intraganglionic injection of 2×10^{10} viral particles of AAV6-CMV-EGFP induced highly efficient EGFP expression in all subpopulations of DRG neurons (Supporting Fig. 3a, b). In contrast, an equivalent dose of AAV6-GFAP-EGFP resulted in EGFP expression in ring-like immunopositivity surrounding the Tubb3-labled primary sensory neuron somata, with EGFP signals residing outside of NKAα1-labeled neuronal plasma membranes, but highly colocalized with GFAP staining (Fig. 1). To estimate the rate of SGC transduction after vector injection, we used immunohistochemical detection of the SGC-ring surround the neurons. For DRGs injected with AAV6-GFAP-EGFP, EGFP-positive SGC rings were observed surrounding 67±11% of neurons while only few neuron somata (~1%) with EGFP positivity were observed (see below in Fig. 7 for details). These results indicate that the GFAP promoter restricted AAV-mediated transgene expression almost exclusively to the perisomatic sheath of GFAP-labeled SGCs, though a low transgene expression was still observed in neurons. A second estimation of glial transduction rates was performed in SGCs clearly identified as such by their costaining for SGC markers and the presence of a distinct SGC nucleus adjacent to a neuronal soma profile (Nascimento et al., 2014; Puljak et al., 2009). Examining only the EGFP fluorescence immediately surrounding the SGC nucleus avoids the ambiguities of counting areas where cytoplasm is minimal, which makes transduction hard to confirm by fluorescence, and which makes SGC enumeration impossible because their processes overlap. Among these clearly identified SGCs, transduction rates by AAV6-GFAP-EGFP were 70±8% (n=4 DRG sections, total 598 SGCs) using GFAP for identification and 72±6% using GS for identification (n=4 DRG sections, total 1107 SGCs; Supporting Fig. 4).

Additional confirmation of SGC localization of transgene expression transferred by AAV6-GFAP-EGFP was obtained through costaining of EGFP with other glial cell markers for SGCs including Vimentin, GS, $K_{ir}4.1$, EAAT1, and Hmgcs1, and with SGCs/Schwann cell co-positive marker S100, as well as with Iba1 for microglial cells (Wang et al., 2016). Results showed (compared to the negative IHC controls shown in Supporting Fig 2b) that GFAP promoter-driven EGFP expression was colabeled with each of the SGC markers but colocalization was not evident with Iba1 (Fig. 2a). We also used the intensity correlation

analysis (ICA) method to quantitatively evaluate the co-expression of EGFP with Hmgcs1 (SGC marker) and EGFP with Iba1 (microglia marker). Notably, plot profile and colocalization analysis (Fig. 3) revealed dependent staining, i.e. colocalization, between EGFP and Hmgcs1 (ICQ of 0.219±0.013; n=ROIs in 4 different DRGs), but not between EGFP and Iba1 (ICQ of −0.19±0.013 (n=ROIs in 4 different DRGs). These data add further support to the view that AAV with GFAP promoter drives transgene expressed in SGCs but not microglia.

In sections 5 weeks post injection of AAV6-GFAP-EGFP, transgene expression was also observed in the sciatic nerve (Fig. 2b) and intrathecal nerve roots (data not shown), but EGFP was not costained with MBP, a marker of myelin. It is reported that GFAP expression is repressed in Schwann cells that form myelin and, after birth, only non-myelin-forming Schwann cells and Schwann cells that dedifferentiate after nerve injury express GFAP (Jessen et al., 1984; Triolo et al., 2006). These findings indicate that the AAV6-GFAP-EGFP vector drives transgene expression selectively in SGCs and nonmyelinating Schwann cells.

We next examined whether EGFP expression in the SGCs could trigger an inflammatory response in SGCs and induce adverse effects upon sensory behavioral performance following intraganglionic injection of AAV6-GFAP-EGFP. We therefore quantitatively analyzed GFAP protein expression by western blots on DRG tissues from animals that received AAV6-GFAP-EGFP injection, from animals subjected to sham-injection (i.e. DRG exposure but no injection), or from naive animals with no surgery. Results showed no significant difference of GFAP protein levels in the DRGs 5 weeks post injection with AAV6-GFAP-EGFP compared to naive or sham-operated DRGs ($F_{3,14}$=0.6126, p>0.05, Fig. 4a). We also did not observe any positive cells immunolabeled by CD6, a pan-T cell marker, or CD8, a cytotoxic T-cell marker, using lymph node tissue as a positive control (data not shown). These results suggest that vector injection and selective EGFP expression in SGCs did not induce marked inflammatory response in the ganglia. Furthermore, injection of AAV6-GFAP-EGFP into L4 and L5 DRGs did not alter mechanical (vF: all assigned a score of 25 g) or thermal (Heat: $F_{2,9}$=0.3805, p>0.05) sensitivity of the ipsilateral plantar skin during the 5 weeks postinjection observation period (Fig. 4b).

AAV vectors with CMV promoter and packaged into AAVshH10 and AAVshH19 produce neuron-restricted gene expression

AAVshH10 and AAVshH19 are engineered capsid variants with Muller glia-prone transduction after intravitreal application (Klimczak et al., 2009; Koerber et al., 2009). To test whether cell-specificity for the SGC transduction in DRG could be enhanced by AAVshH10-CMV-EGFP and AAVshH19-CMV-EGFP in DRGs, we delivered 2×10^{10} genome copy of either vector into the L4 and L5 DRGs (n=4 rat per vector), and the cell-specificity of *in vivo* transduction was compared to AAV6-CMV-EGFP. Immunofluorescent analyses revealed robust EGFP expression in DRG neurons by both AAVshH10-CMV-EGFP and AAVshH19-CMV-EGFP, using a pan neuronal marker Tubb3 (Supporting Fig. 3c–f) or NKAlα (Fig. 5) to identify neuronal somata. AAVshH10-CMV-EGFP showed extensive colocalization of EGFP to all-sized neurons, similar to AAV6-CMV-EGFP, while AAVshH19-CMV-EGFP preferentially labeled large-sized neurons (similar to AAV2-CMV-

EGFP, data not shown). No significant SGC transduction costained by GFAP after AAV6-CMV-EGFP, AAVshH10CMV-EGFP, or AAVshH19-CMV-EGFP injections regardless of the pseudotypes employed (Fig. 5). These results indicate that the altered capsid residues in AAVshH10 and AAVshH19 capsids did not modulate the neuronal tropism of these vectors when used in the DRG. We also prepared AAVshH10-GFAP-EGFP and injected (2×10^{10} GC particles) into L4/L5 DRGs (n=4 rats), after which *in vivo* transduction was analyzed 5wk later by IHC. This showed that this construct also induced efficient transgene expression selectively to SGCs (Fig. 6), similar to AAV6-GFAP-EGFP.

Comparison of the transduction properties of all five vectors (Fig. 7) shows that both AAV6-GFAP-EGFP and AAVshH10-GFAP-EGFP produce efficient SGC-selective transgene expression whereas AAV6-CMV-EGFP, AAVshH10-CMV-EGFP, and AAVshH19-CMV-EGFP fail to transduce SGCs ($F_{4,20}$=33.5, p<0.001, Fig. 7a). In contrast, AAV6-GFAP-EGFP and AAVshH10-GFAP-EGFP produce limited neuronal transduction while AAVs using CMV promoters (AAV6-, shH10-, shH19-CMV-EGFP) produce robust neuronal transduction ($F_{4,34}$ =18.58, p<0.001, Fig. 7b).

Effective delivery of two transgenes to SGCs and neurons separately by dual AAV vectors

This study was designed to examine the strategy of using two simultaneously applied AAV vectors to separately express distinct transgenes in SGCs vs. neurons, expressing EGFP driven by a GFAP promoter to identify SGC expression and mCherry driven by a CMV promoter to identify neuronal expression, with these two vectors being packaged otherwise identical. We first tested the specificity of anti-GFP and anti-mCherry antibodies in detecting individual fluorescent proteins. To this end, HEK293 cells were infected with the AAV6-GFAP-EGFP or AAV6-CMV-eCherry (multiplicity of infection: 10^5 GC/cell of each vector). Cell lysates 48 hours after infection were analyzed by Western blots with anti-GFP or anti-mCherry. This resulted in the expression of individual protein of the expected size, with no cross-reactivity observed for both the anti-GFP and anti-mCherry antibodies (Fig. 8a).

In the co-delivery experiments performed *in vivo*, dual AAV vectors composing of AAV6-GFAP-EGFP and AAV6-CMV-mCherry at 1:1 ratio mixture were injected into L4/L5 DRGs (n=4 rats). Immunofluorescent analyses of DRG sections at 5 weeks after injection revealed EGFP-expressing SGCs and mCherry-expressing neurons without evidence of coexpression (Fig. 8b and c). Quantitative estimation of transduction rates (4 DRGs) showed 40±8% EGFP-positive SGC rings and 34±11% mCherry-positive neuron soma. These results indicate that this dual AAV strategy is successful in driving selective expression in DRG neurons *versus* SGCs using a GFAP promoter to express one transgene in SGCs while using CMV promoter to target another transgene expression only in neurons.

DISCUSSION

SGCs represent a predominant glial cell type in the DRG, host a complex network of signaling pathways, and are recognized as an important sensory component and mediators in pain sensation (Pannese, 2010; Wang et al., 2016). Development of a SGC permissive AAV vector would be valuable for expanding the utility of AAV in modeling and treating in chronic pain. *In vitro* studies show efficient glial cell transduction for all serotype AAV

vectors (Howard et al., 2008) and a number of AAV serotypes has shown variable glial tropism *in vivo* in various neural tissues by different routes of application (Aschauer et al., 2013; Koerber et al., 2009; Mason et al., 2010; Petrosyan et al., 2014; Samaranch et al., 2013; Wollmann et al., 2005; Yu et al., 2013). However, the results have not translated into reliable, specific, and widespread transduction of SGCs in the DRG.

In this study, we evaluated the specificity and efficiency of targeting SGCs relative to primary sensory neurons, using AAV vectors incorporating either a GFAP promoter or a constitutively active CMV promoter. The data demonstrate that the AAV with a GFAP promoter was capable of discriminating for SGC transduction. Our data show that transgene expression was highly selective for SGCs and virtually absent in microglia, neurons, or myelinating Schwann cells when AAVs delivered to DRG controlled transgene expression by the GFAP promoter. Further study is needed to determine whether administration of this GFAP promoter vector by various routes (intraganglionic, intraspinal, or intrathecal) or at different timepoints (immediately or delayed) after nerve injury might be capable of targeting and controlling the highly proliferated glial cell population that follows nerve injury in neuropathic pain (Ji et al., 2013).

We also examined cell specificity of AAVs packaged by use of recently engineered “Müller glia-prone” capsids AAVshH10, an AAV6 variant that is highly homologous to its parent AAV6 with only four different capsid residues, and AAVshH19, an AAV2 variant that is a chimera composed of capsid regions from several serotypes swapped into AAV2. Previous reports show substantially increased transduction of Müller glial cells by these capsid variants when applied by intravitreal route, compared to AAV6 and AAV2 controls (Vandenberghe and Auricchio, 2012). Our results showed that a single intraganglionic injection of AAVshH10 or AAVshH19 carrying a CMV-EGFP cassette induced highly efficient, selective transduction of sensory neurons, but no significant enhancement in transduction of SGCs. This indicates that, although the divergent capsid residues in AAVshH10 and AAVshH19 may act in concert to improve glia transduction in visual system or brain glioma (Byrne et al., 2013; Klimczak et al., 2009; Koerber et al., 2009; Pellissier et al., 2014; Vacca et al., 2016), this shift in tropism does not occur when applied into DRG. Nonetheless, the capsid variants of shH10 and shH19 may be considered for use as viable alternatives to AAV6 and AAV2 for efficient neuronal transduction in DRGs.

A unique characteristic of DRG structure is that SGCs tightly ensheathe the somata of primary sensory neurons to form discrete anatomical and functional sensory units (Pannese, 2010; Wang et al., 2016). Bidirectional neuron-SGC communication plays an essential role in regulating afferent signaling (Huang et al., 2013; Kim et al., 2016; Rozanski et al., 2013; Zhang et al., 2015). Understanding the complex neuron-SGC communication in normal and injured DRG relies on the availability of experimental systems to separately target primary sensory neurons and SGCs *in vivo*. Therefore, AAV vectors with high, equivalent, and reliable tropism for both primary sensory neurons and SGCs will be valuable but are yet to be identified. We have demonstrated that a dual AAV strategy using two vectors, one with GFAP promoter and the other with CMV promoter, enabled efficiently expression of transgenes selectively in neurons vs. SGCs. The ability to target gene transfer selectively to SGCs and neurons by this dual AAV strategy may provide a useful approach for

investigations of mechanistic neuron-SGC communication and also aid in the development of novel therapeutic strategies targeting primary sensory neuron and SGCs.

In summary, this report, together with our prior studies (Yu et al., 2013; Yu et al., 2016), demonstrate that the GFAP promoter, but not capsid divergence, offer an efficient pathway for selective gene expression in SGCs following intraganglionic AAV delivery in adult rats. A dual AAV system, one with GFAP promoter and the other with CMV promoter, can efficiently express transgenes selectively in neurons vs. SGCs. Future research may develop the therapeutic potential of GFAP promoter AAV in targeting SGC signaling for chronic pain.

Supplementary Material

Refer to Web version on PubMed Central for supplementary material.

Acknowledgments

The authors would like to thank Dr. David V. Schaffer (University of California, Berkeley) for providing the AAVshH10 and AAVshH19 plasmids. Our grateful thanks go to Gregory Fischer for his technical assistance.

Grant information: This work was supported in part by the grants from the Department of Veterans Affairs Rehabilitation Research and Development (I01RX001940, QH), the Advancing a Healthier Wisconsin (FP00005706, QH and HY), and the National Institute of Neurological Disorders and Stroke (R01NS079626-01, QH).

References

Aschauer DF, Kreuz S, Rumpel S. Analysis of transduction efficiency, tropism and axonal transport of AAV serotypes 1, 2, 5, 6, 8 and 9 in the mouse brain. PloS one. 2013; 8:e76310. [PubMed: 24086725]

Asokan A, Schaffer DV, Samulski RJ. The AAV vector toolkit: poised at the clinical crossroads. Molecular therapy:the journal of the American Society of Gene Therapy. 2012; 20:699–708. [PubMed: 22273577]

Beutler AS, Reinhardt M. AAV for pain: steps towards clinical translation. Gene Ther. 2009; 16:461–9. [PubMed: 19262609]

Beutler AS. AAV provides an alternative for gene therapy of the peripheral sensory nervous system. Molecular therapy:the journal of the American Society of Gene Therapy. 2010; 18:670–3. [PubMed: 20357781]

Byrne LC, et al. AAV-mediated, optogenetic ablation of Muller Glia leads to structural and functional changes in the mouse retina. PLoS One. 2013; 8:e76075. [PubMed: 24086689]

Chaplan SR, et al. Quantitative assessment of tactile allodynia in the rat paw. Journal of neuroscience methods. 1994; 53:55–63. [PubMed: 7990513]

Chen Y, et al. Activation of P2X7 receptors in glial satellite cells reduces pain through downregulation of P2X3 receptors in nociceptive neurons. Proc Natl Acad Sci U S A. 2008; 105:16773–8. [PubMed: 18946042]

Dalkara D, et al. AAV mediated GDNF secretion from retinal glia slows down retinal degeneration in a rat model of retinitis pigmentosa. Mol Ther. 2011; 19:1602–8. [PubMed: 21522134]

Fischer G, et al. Direct injection into the dorsal root ganglion: technical, behavioral, and histological observations. J Neurosci Methods. 2011; 199:43–55. [PubMed: 21540055]

Gao YJ, Ji RR. Targeting astrocyte signaling for chronic pain. Neurotherapeutics:the journal of the American Society for Experimental NeuroTherapeutics. 2010; 7:482–93. [PubMed: 20880510]

Hanani M. Satellite glial cells in sensory ganglia:from form to function. Brain Res Brain Res Rev. 2005; 48:457–76. [PubMed: 15914252]

Howard DB, et al. Tropism and toxicity of adeno-associated viral vector serotypes 1, 2, 5, 6, 7, 8, and 9 in rat neurons and glia in vitro. Virology. 2008; 372:24–34. [PubMed: 18035387]

Huang LY, Gu Y, Chen Y. Communication between neuronal somata and satellite glial cells in sensory ganglia. Glia. 2013; 61:1571–81. [PubMed: 23918214]

Jasmin L, et al. Can satellite glial cells be therapeutic targets for pain control? Neuron glia biology. 2010; 6:63–71. [PubMed: 20566001]

Jessen KR, Thorpe R, Mirsky R. Molecular identity, distribution and heterogeneity of glial fibrillary acidic protein: an immunoblotting and immunohistochemical study of Schwann cells, satellite cells, enteric glia and astrocytes. J Neurocytol. 1984; 13:187–200. [PubMed: 6726286]

Ji RR, Berta T, Nedergaard M. Glia and pain: is chronic pain a gliopathy? Pain. 2013; (154 Suppl 1):S10–28. [PubMed: 23792284]

Kim DS, et al. Profiling of dynamically changed gene expression in dorsal root ganglia post peripheral nerve injury and a critical role of injury-induced glial fibrillary acidic protein in maintenance of pain behaviors [corrected]. Pain. 2009; 143:114–22. [PubMed: 19307059]

Kim YS, et al. Coupled Activation of Primary Sensory Neurons Contributes to Chronic Pain. Neuron. 2016; 91:1085–96. [PubMed: 27568517]

Klimczak RR, et al. A novel adeno-associated viral variant for efficient and selective intravitreal transduction of rat Muller cells. PloS one. 2009; 4:e7467. [PubMed: 19826483]

Koerber JT, et al. Molecular evolution of adeno-associated virus for enhanced glial gene delivery. Molecular therapy:the journal of the American Society of Gene Therapy. 2009; 17:2088–95. [PubMed: 19672246]

Lee Y, et al. GFAP promoter elements required for region-specific and astrocyte-specific expression. Glia. 2008; 56:481–93. [PubMed: 18240313]

Li Q, et al. A syntaxin 1, Galpha(o), and N-type calcium channel complex at a presynaptic nerve terminal:analysis by quantitative immunocolocalization. J Neurosci. 2004; 24:4070–81. [PubMed: 15102922]

Liu F, Yuan H. Role of glia in neuropathic pain. Frontiers in bioscience. 2014; 19:798–807.

Mason MR, et al. Comparison of AAV serotypes for gene delivery to dorsal root ganglion neurons. Mol Ther. 2010; 18:715–24. [PubMed: 20179682]

McMahon SB, Malcangio M. Current challenges in glia-pain biology. Neuron. 2009; 64:46–54. [PubMed: 19840548]

Milligan ED, Watkins LR. Pathological and protective roles of glia in chronic pain. Nature reviews. Neuroscience. 2009; 10:23–36. [PubMed: 19096368]

Nascimento DS, Castro-Lopes JM, Moreira Neto FL. Satellite glial cells surrounding primary afferent neurons are activated and proliferate during monoarthritis in rats: is there a role for ATF3? PLoS One. 2014; 9:el08152.

Ohara PT, et al. Evidence for a role of connexin 43 in trigeminal pain using RNA interference in vivo. J Neurophysiol. 2008; 100:3064–73. [PubMed: 18715894]

Pannese E. The structure of the perineuronal sheath of satellite glial cells (SGCs) in sensory ganglia. Neuron glia biology. 2010; 6:3–10. [PubMed: 20604977]

Pellissier LP, et al. Specific tools for targeting and expression in Muller glial cells. Mol Ther Methods Clin Dev. 2014; 1:14009. [PubMed: 26015954]

Petrosyan HA, et al. Transduction efficiency of neurons and glial cells by AAV-1, -5, -9, -rh10 and -hu11 serotypes in rat spinal cord following contusion injury. Gene therapy. 2014; 21:991–1000. [PubMed: 25119378]

Puljak L, et al. Lidocaine injection into the rat dorsal root ganglion causes neuroinflammation. Anesth Analg. 2009; 108:1021–6. [PubMed: 19224819]

Rozanski GM, et al. Low voltage-activated calcium channels gate transmitter release at the dorsal root ganglion sandwich synapse. The Journal of physiology. 2013; 591:5575–83. [PubMed: 24000176]

Samaranch L, et al. Strong cortical and spinal cord transduction after AAV7 and AAV9 delivery into the cerebrospinal fluid of nonhuman primates. Hum Gene Ther. 2013; 24:526–32. [PubMed: 23517473]

Scholz J, Woolf CJ. The neuropathic pain triad:neurons, immune cells and glia. Nat Neurosci. 2007; 10:1361–8. [PubMed: 17965656]

Triolo D, et al. Loss of glial fibrillary acidic protein (GFAP) impairs Schwann cell proliferation and delays nerve regeneration after damage. J Cell Sci. 2006; 119:3981–93. [PubMed: 16988027]

Vacca O, et al. AAV-mediated gene therapy in Dystrophin-Dp71 deficient mouse leads to blood-retinal barrier restoration and oedema reabsorption. Hum Mol Genet. 2016; 25:3070–3079. [PubMed: 27288449]

Vandenberghe LH, Auricchio A. Novel adeno-associated viral vectors for retinal gene therapy. Gene Ther. 2012; 19:162–8. [PubMed: 21993172]

Vit LP, et al. Silencing the Kir4.1 potassium channel subunit in satellite glial cells of the rat trigeminal ganglion results in pain-like behavior in the absence of nerve injury. J Neurosci. 2008; 28:4161–71. [PubMed: 18417695]

von Jonquieres G, et al. Glial promoter selectivity following AAV-delivery to the immature brain. PLoS One. 2013; 8:e65646. [PubMed: 23799030]

Wang F, et al. HMG-CoA synthase isoenzymes 1 and 2 localize to satellite glial cells in dorsal root ganglia and are differentially regulated by peripheral nerve injury. Brain Res. 2016; 1652:62–70. [PubMed: 27671501]

Watkins LR, Maier SF. Glia: a novel drug discovery target for clinical pain. Nature reviews. Drug discovery. 2003; 2:973–85. [PubMed: 14654796]

Wollmann G, Tattersall P, van den Pol AN. Targeting human glioblastoma cells: comparison of nine viruses with oncolytic potential. Journal of virology. 2005; 79:6005–22. [PubMed: 15857987]

Yu H, et al. Lentiviral gene transfer into the dorsal root ganglion of adult rats. Mol Pain. 2011; 7:63. [PubMed: 21861915]

Yu H, et al. Intraganglionic AAV6 Results in Efficient and Long-Term Gene Transfer to Peripheral Sensory Nervous System in Adult Rats. PloS one. 2013; 8:e61266. [PubMed: 23613824]

Yu H, Fischer G, Hogan QH. AAV-Mediated Gene Transfer to Dorsal Root Ganglion. Methods Mol Biol. 2016; 1382:251–61. [PubMed: 26611592]

Zhang Y, et al. Identifying local and descending inputs for primary sensory neurons. J Clin Invest. 2015; 125:3782–94. [PubMed: 26426077]

Zolotukhin I, et al. Improved Adeno-associated Viral Gene Transfer to Murine Glioma. J Genet Syndr Gene Ther. 2013:4.

Significance statement

SGCs represent a predominant glial cell type in the DRG. Development of a selective SGC permissive AAV vector is a current challenge but would be valuable for expanding the utility of AAV in modeling and treating in chronic pain. Our work establishes that GFAP promoter is effective in providing SGC-selective transgene expression following intraganglionic AAV delivery in adult rats, and this strategy should prove useful for the development of gene expression systems targeting SGC signaling for chronic pain.

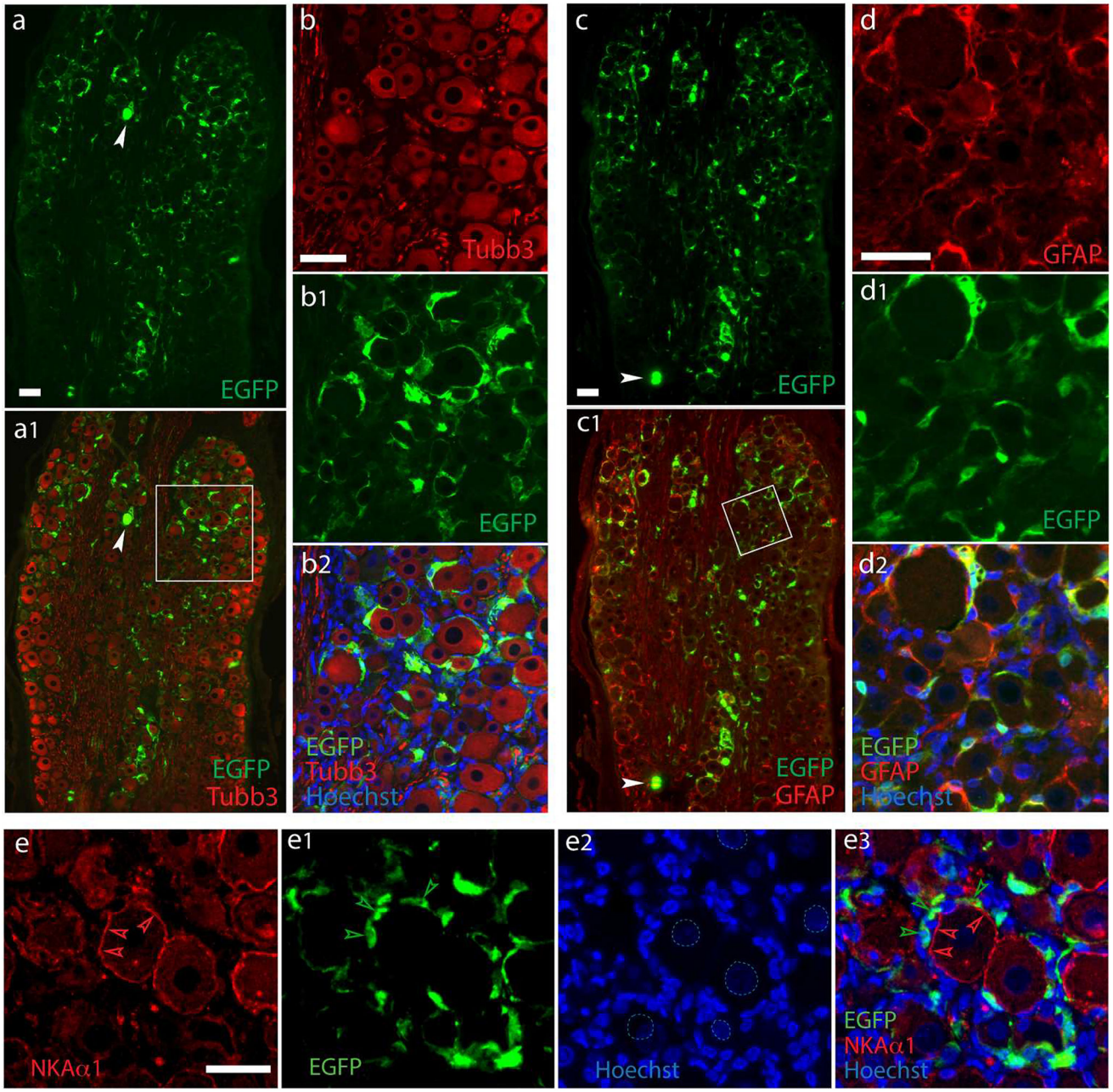

Figure 1. SGC-specific transduction after intraganglionic injection of AAV6-GFAP-EGFP

Representative images from DRGs assessed 5 weeks after injection of 2.0×10^{10} GC per DRG of AAV6-GFAP-EGFP. Data are representatives of 6 DRGs from three rats. High-efficient EGFP expression was found clustered in ring-like arrangements (**a**) around the majority of DRG neurons of all subpopulation labeled by a pan-neuron maker Tubb3 (**a1**). Only few neuronal somata with EGFP positivity are occasionally observed (arrowheads). The boxed area of al is shown at higher magnification as Tubb3 (**b**), EGFP (**b1**), and merged (**b2**) images. In contrast, double labeling demonstrates clear overlay of EGFP with the SGCs labeled by GFAP (**c** and **c1**, with the boxed area of c1 shown at higher magnification as GFAP (**d**), EGFP (**d1**), and merged (**d2**) images)). EGFP signals resides clearly outside of

NKAα1-labeled neuronal plasma membranes (e to e3; dashed circles in e2 outline less intensively Hoechst-stained neuronal nuclei compared with SGC nuclei, as are typically seen). Scale bars: 100μm for all.

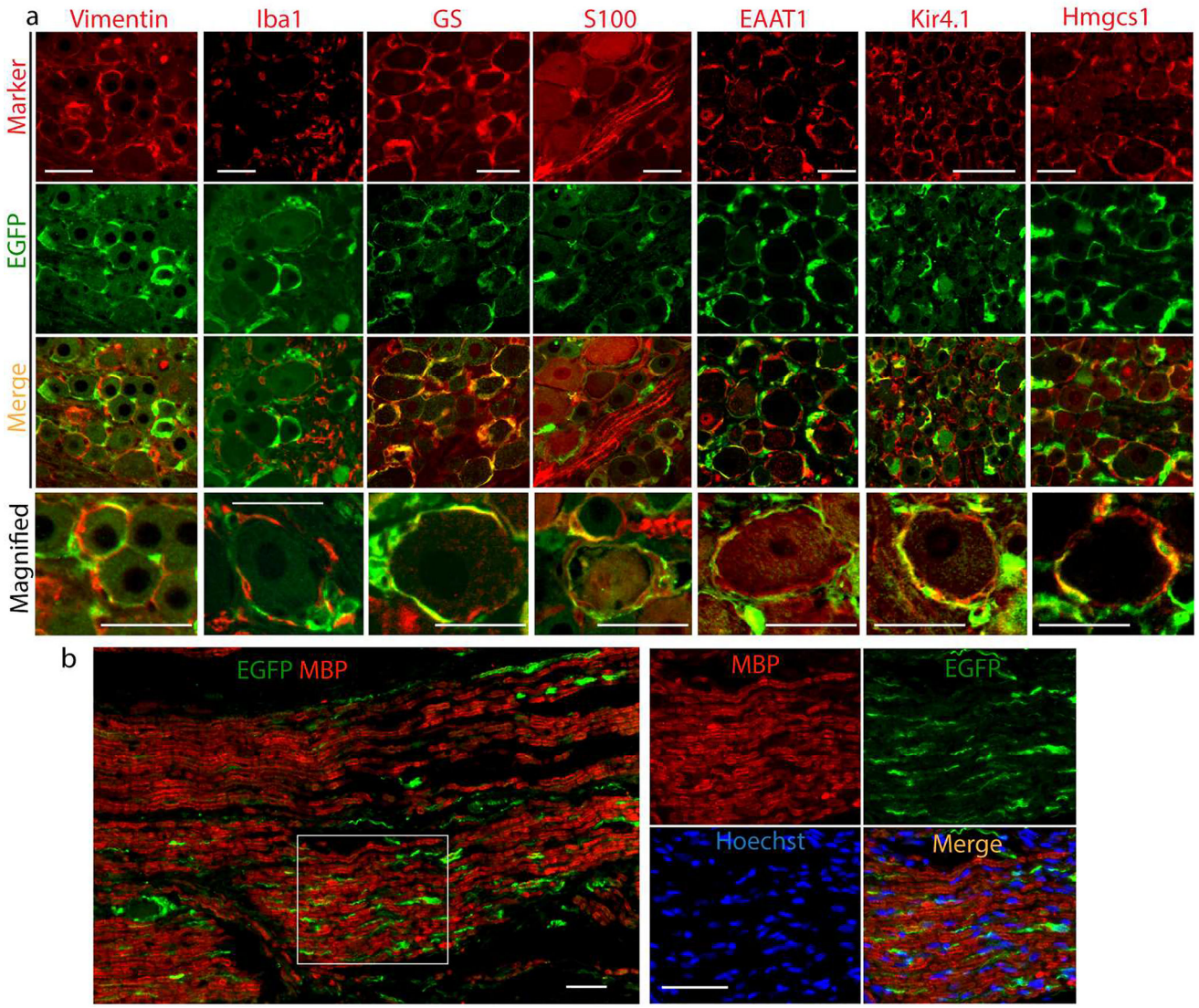

Figure 2. Colocalization of GFAP promoter AAV6-mediated EGFP expression with glial cell markers

(**a**) Representative results of double immunolabeling of EGFP with multiple authentic glial cell markers (Vimentin, Iba1, GS, S100, EAAT1, Kir4.1, and Hmgcs1) labeled on the top and filtering (marker, EGFP, or merge) indicated at the left of the panels, (**b**) EGFP expression was observed in the section of sciatic nerve, but EGFP was not costained with MBP, a marker of myelin. Right panels are magnified inset of b). Scale bar: 100μm for all panels.

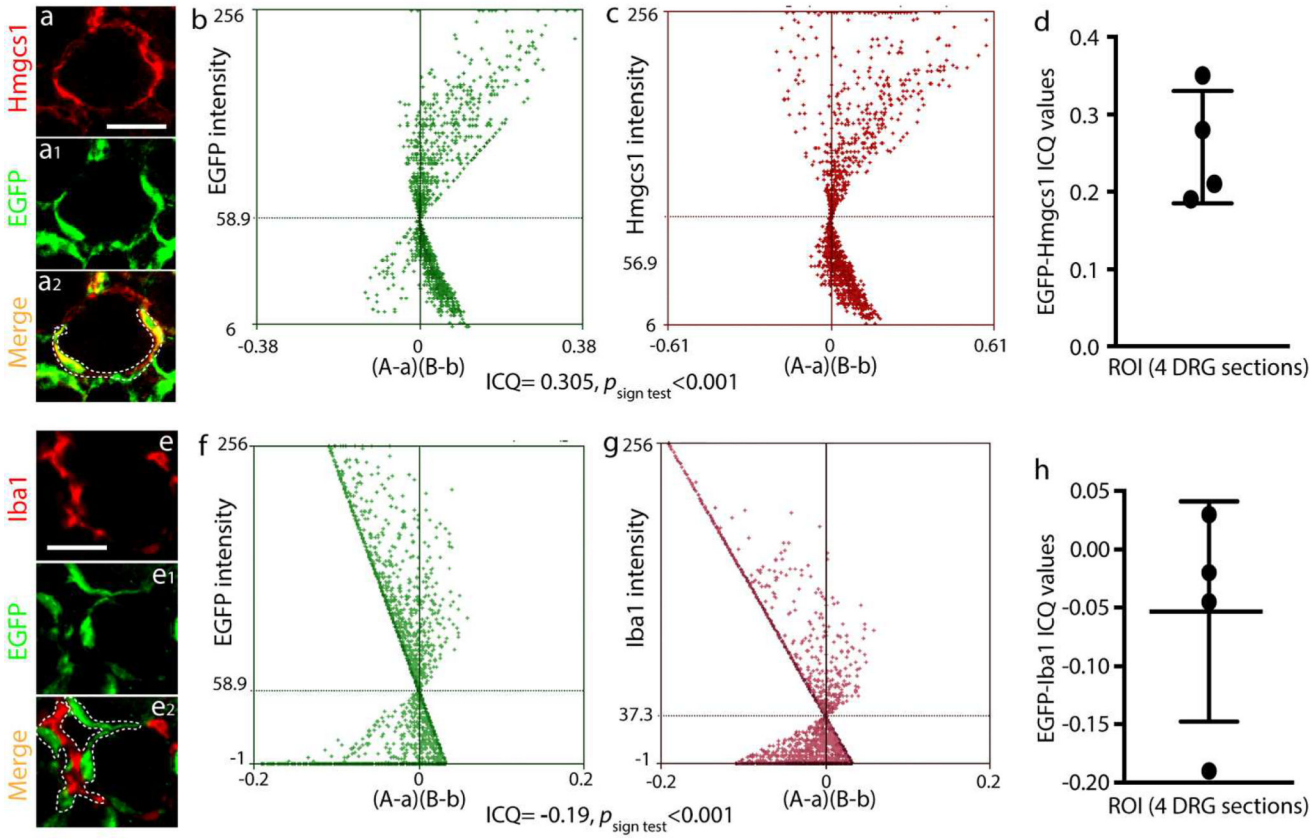

Figure 3. Intensity correlation analysis of EGFP with Hmgcs1 or Iba1

Pseudocolor images of a representative DRG section 5 weeks after AAV6-GFAP-EGFP injection labeled with Hmgcs1 (**a**) and EGFP (**a1**), with the merged image (**a2**) showing co-labeling (yellow). Scatter plots for the region demarcated by the white dashed line in a2 show strong right skewing for EGFP (**b**) and Hmgcs1(**c**). In these panels, “A” is the intensity of EGFP while “a” is the average of these values, and “B” is the intensity of Hmgcs1 while “b” is the average of these values. For this region, the ICQ value is 0.28 (P<0.001). ICQ values (**d**) for EGFP/Hmgcs1 staining of matched ROIs (the green and red colors varied in close synchrony) (n=4 DRGs). EGFP colabeling with Iba1did not found colocalization (**e** to **e2**). Scatter plots for the region outlined by the white dashed line in e2 show strong left skewing for EGFP (**f**) and Iba1 (**g**). In these panels, “A” is the intensity of EGFP while “a” is the average of these values, and “B” is the intensity of Iba1 while “b” is the average of these values. The ICQ value for the region = −0.19 (P<0.001). ICQ values (**h**) for EGFP/Iba1 staining of matched ROIs (n=4 DRGs). Scale bar: 100μm for all panels.

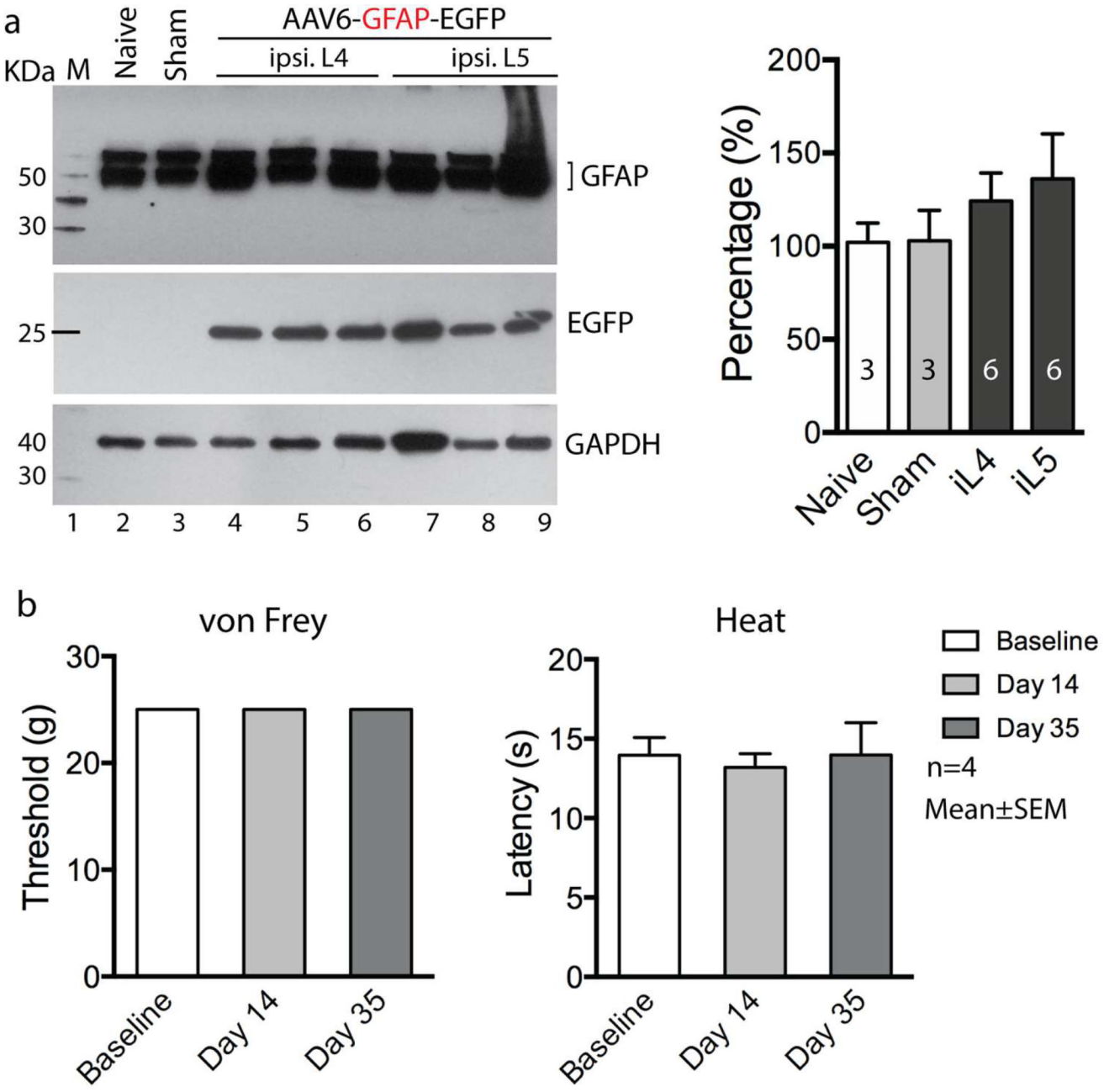

Figure 4. GFAP western and sensory evaluation after AAV6-GFAP-EGFP injection into DRGs

(**a**) Representative immunoblots of GFAP (top panel), EGFP (middle panel), and GAPDH (bottom panel) on the lysates of the DRGs from a naïve L4 DRG (lane 2), a L5 DRG from sham-operated rat (lane 3), as well as three L4 DRGs (lane 4, 5 and 6) and three L5 DRGs (lane 7, 8 and 9) harvested at 5-week after injected with AAV6-GFAP-EGFP. Arrows point to the expected size bands for GFAP, EGFP, and GAPDH as a loading control. Bar chart in the right panel is the results of densitometry analysis. Group comparisons showed no significant differences. (**b**) Sensory sensitivity evaluated by the von Frey (left panel) and Heat (Hargreaves, right panel) tests at baseline, day 14, and day 35 after AAV6-GFAP-EGFP in non-injured rats (n = 4 rats).

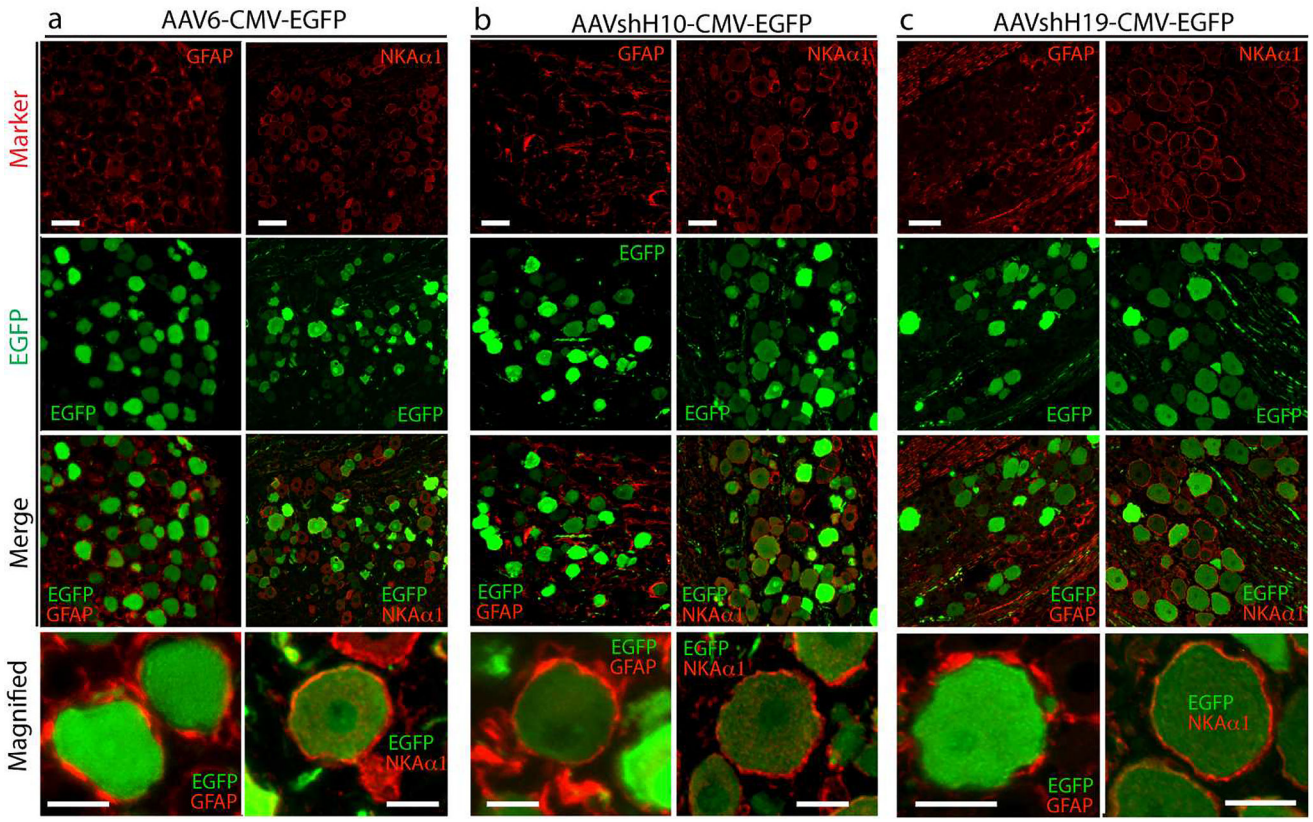

Figure 5. Transduction profile after intraganglionic injection of AAVshH10-CMV-EGFP or AAVshH19-CMV-EGFP

Double immunostaining of EGFP (green) with GFAP (red, in left panel) or NKAα1 (red in right panel) in DRG sections after injection of AAV6-CMV-EGFP (AAV6, **a**), AAVshH10-CMV-EGFP (AAVshH10, **b**), and AAVshH19-CMV-EGFP (AAVshH19, **c**) into DRGs of non-injured rats, showing preferential neuronal transduction of all three vectors. Scale bar: 100μm for all panels.

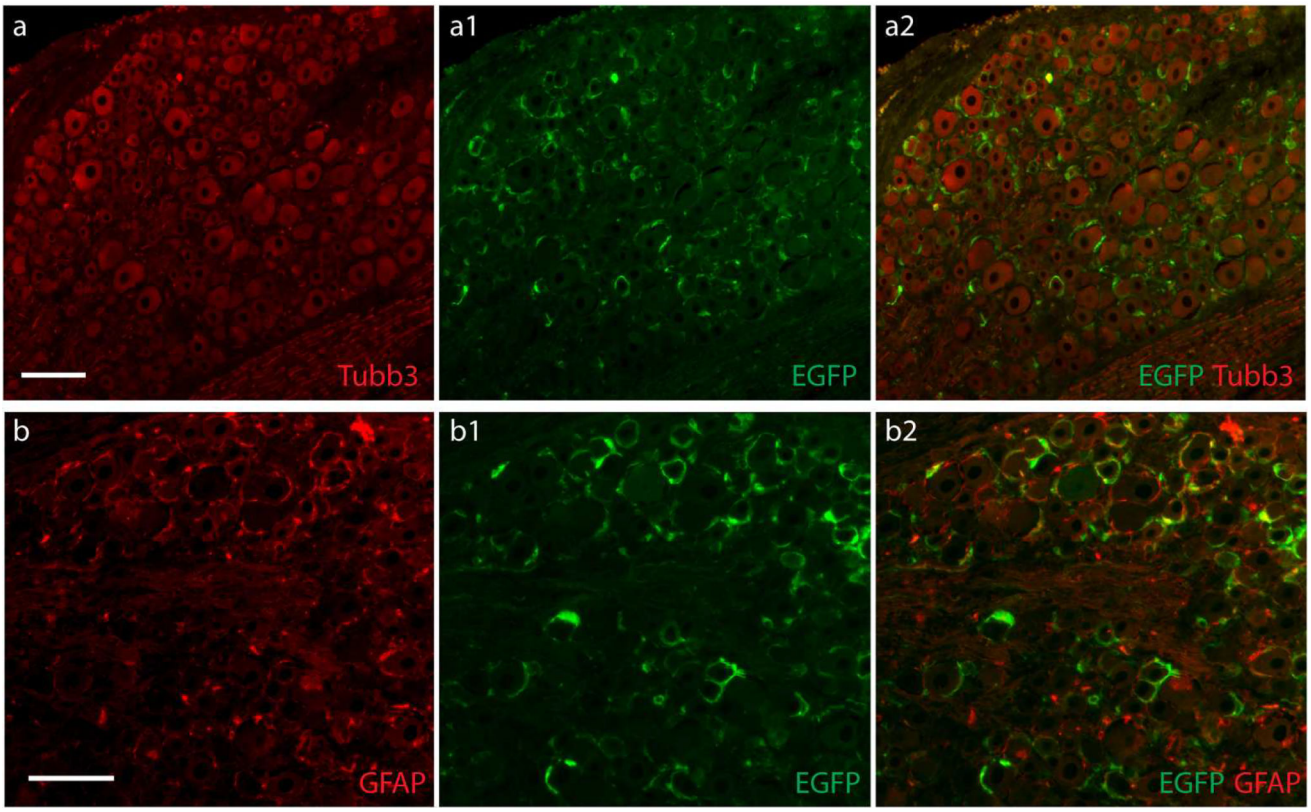

Figure 6. SGC transduction after intraganglionic injection of AAVshH10-GFAP-EGFP

Representative images from DRGs 5 weeks after injection of 2.0×10^{10} GC per DRG of AAVshH10-GFAP-EGFP. Data are representative of 6 DRGs from three rats. Efficient transduction was evident by EGFP expression in SGCs clustered in ring-like arrangements (**a1**) around the majority of DRG neurons labeled by the pan-neuron maker Tubb3 (**a, a2**). Double labeling with GFAP (**b**) demonstrates clear overlay of EGFP (**b1**) with the SGCs labeled by GFAP (**b, b2**). Scale bar: 100μm for all panels.

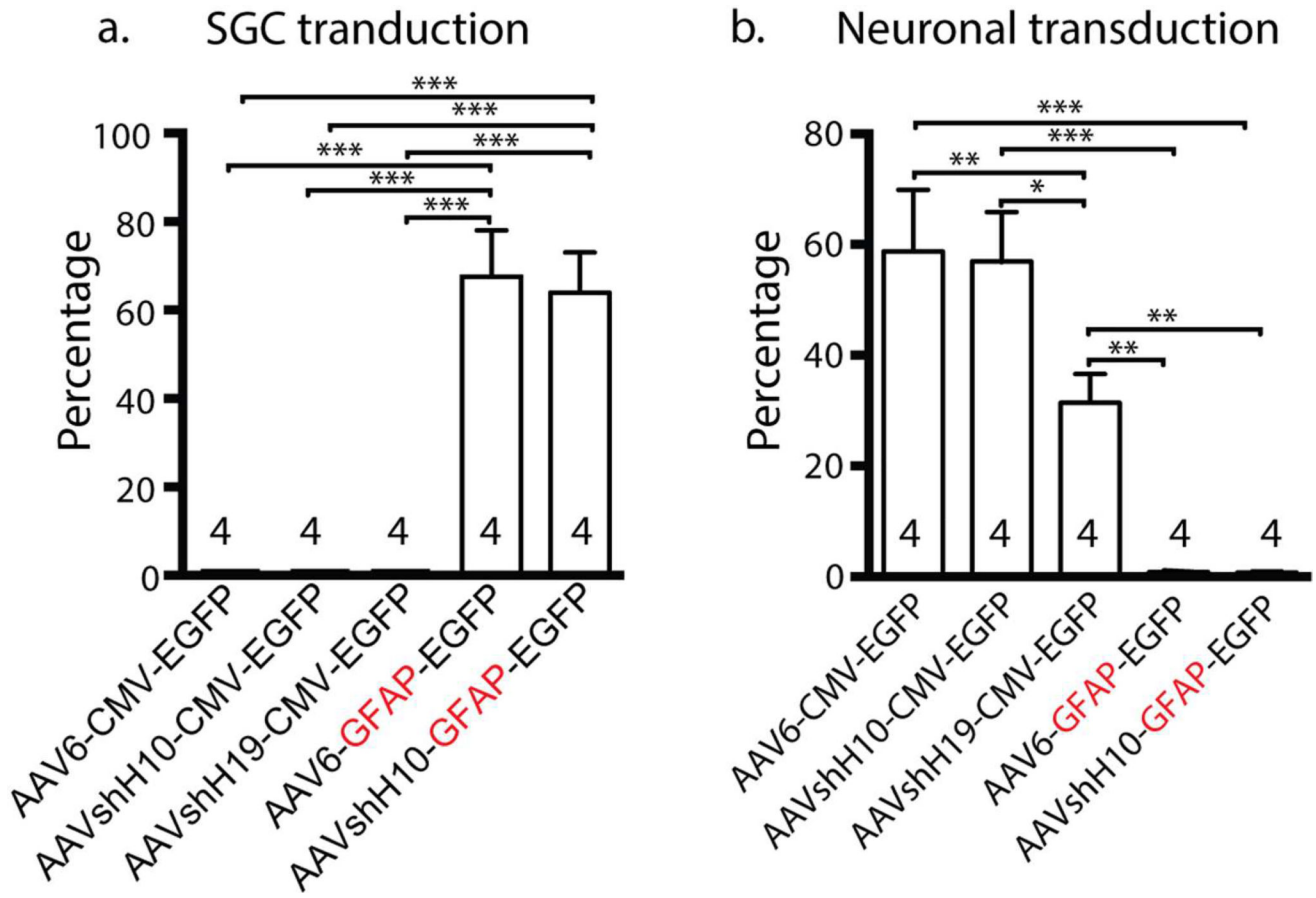

Figure 7. Comparative quantifications of *in vivo* transduction rates of different vectors

(**a, b**) Bar graphs summarize *in vivo* transduction rates of five vectors, ie. AAV6-CMV-EGFP, AAVshH10-CMV-EGFP, AAVshH19-CMV-EGFP, AAV6-GFAP-EGFP, and AAVshH10-GFAP-EGFP. The SGCs transduction rates are shown as the percentage of EGFP-positive SGC rings around all neuronal soma after intraganglionic injection (**a**), and neuronal transduction rates as the percentage of EGFP-positive soma of total neurons (**b**). Mean±SEM, * $p<0.05$, ** $p<0.01$, and *** $p<0.001$.

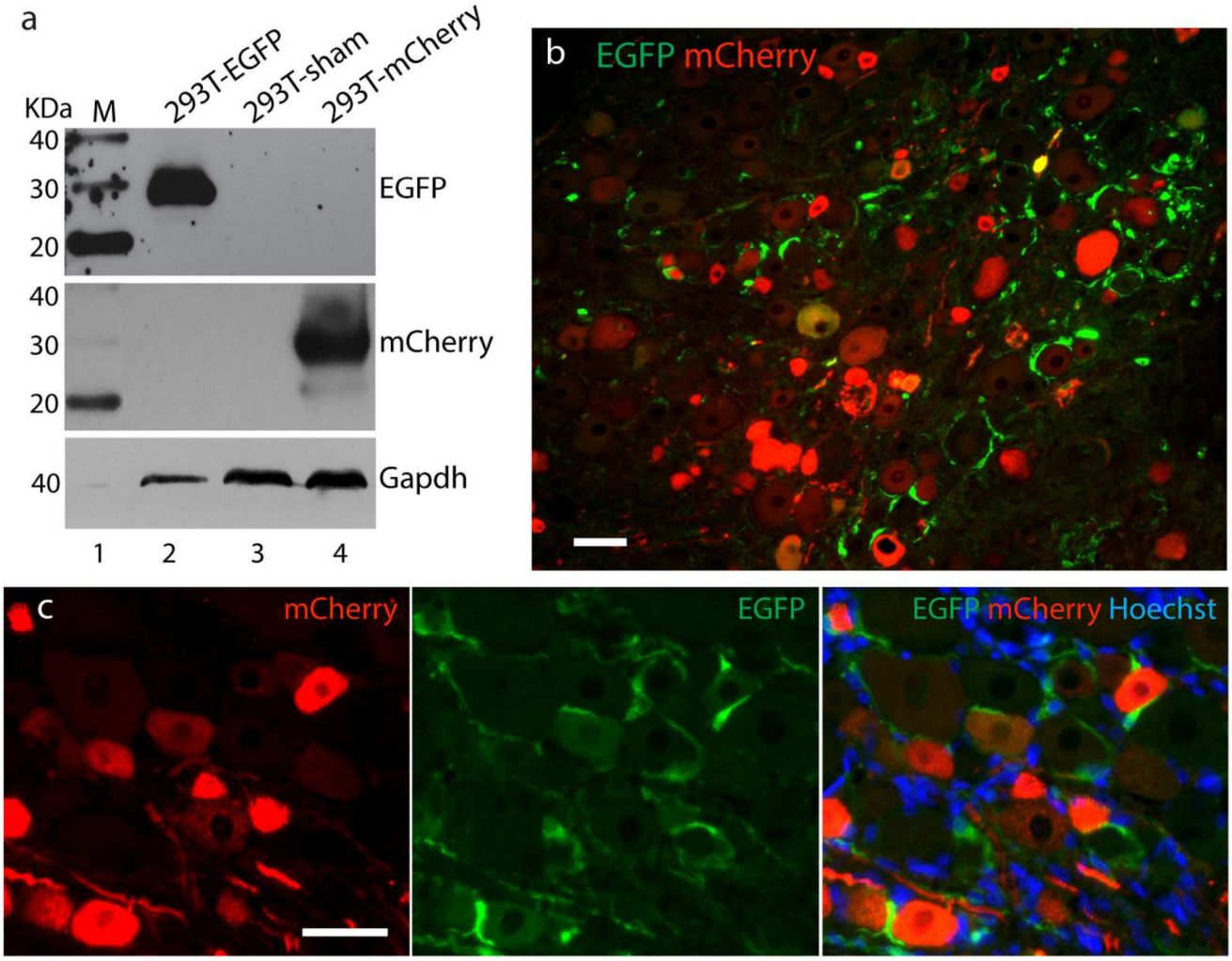

Figure 8. Dual AAVs for selective transduction to neurons vs. SGCs

Western blots with anti-GFP (top), anti-mCherry (middle), and GAPDH (bottom) on the lysates of HEK293 infected with either AAV6-GFAP-EGFP (lane 2) or AAV6-CMV-mCherry (lane 4) show expression of individual protein of the expected size, and no cross-reactivity is observed of anti-GFP antibody with mCherry, or vice versa. Lane 1: protein molecular weight ladders (MagicMark XP Protein Standard, life Technologies). Lane 3: cells transfected with empty pcDNA3.1 plasmid (**a**). Immunofluorescent analyses of DRG sections at 5 weeks after injection of dual vectors reveal EGFP-expressing SGCs and mCherry-expressing neurons (**b** and **c**). Scale bar: 100μm for all panels.

Table 1

Primary antibodies and IgG controls used in this study

Antibody[a]	Host	Supplier/Catalog#[b]	Dilution
GFP	Mouse monoclonal	SCB/sc-32422	1:200 (IHC); 1:400 (Wb)
GFP	Rabbit polyclonal	CS/2555	1:200 (IHC)
mCherry	Rabbit polyclonal	LF/PA534974	1:200 (IHC); 1:400 (Wb)
Hmgcs1	Mouse monoclonal	SCB/sc-393256	1:200 (IHC)
Tubb3	Mouse monoclonal	SCB/sc-80016	1:400 (IHC)
Vimentin	Goat polyclonal	SCB/sc-12886R	1:600 (IHC)
GFAP	Rabbit polyclonal	Dako/Z0334	1:1000 (IHC); 1:2000 (Wb)
GS	Rabbit polyclonal	SCB/sc-6640R	1:600 (IHC)
Iba1	Rabbit polyclonal	Wako/019-19741	1:1000 (IHC)
$K_{ir}4.1$	Guinea pig polyclonal	AlomoneLabs/AGP-012	1:100 (IHC)
EAAT1	Rabbit polyclonal	AlomoneLabs/AGC-021	1:100 (IHC)
S100	Mouse monoclonal	NeoMarkers/MS296Pl	1:200 (IHC)
MBP	Goat polyclonal	SCB/sc-13912	1:1000 (IHC)
GAPDH	Mouse monoclonal	PT/2555	1:2000 (Wb)
CD6	Mouse monoclonal	Millipore/CBL554	1:100 (IHC)
CD8	Mouse monoclonal	Millrpore/217580	1:100 (IHC)
IgG control	Mouse	LF/31903	1:100~400
IgG control	Goat	LF/31245	1:500~1000
IgG control	Rabbit	LF/MA5-16384	1:200~1000

[a] Antibody abbreviations: Hmgcs1, *HMG CoA synthase 1*; Tubb3, *β3-Tubulin*; GFAP, *Glial fibrillary acidic protein*; GS, *Glutamine synthetase*; Iba1, *Ionized calcium binding adaptor molecule 1*; $K_{ir}4.1$, *ATP-sensitive inward rectifier potassium channel 10*; EEAT1, *Excitatory amino acid transporter 1*; S100, *S-100 calcium-binding protein*; MBP, *Myelin basic protein*; *GAPDH*, *Glyceraldehyde 3-phosphate dehydrogenase*; CD6, *Cluster of differentiation 6*; *and* CD8, *Cluster of differentiation 8*.

[b] SCB, Santa Cruz Biotechnology, Santa Cruz, CA; CS, Cell signaling, Danvers, MA; LF, life Technologies, Carlsbad, CA; Dako, Carpintena, CA; Wako, Richmond, VA; Alomone Labs, Jerusalem, Israel; NeoMarkers, Fremont, CA; PT, Proteintech, Rosemont, IL; Millipore, Billenca, MA.